The Influence of Cr Doped TiO_2 on the Optical Property and Photocatalytic Activity under Sunlight Irradiation

Siti Zulaikha Suhaili [1,2*], Muhamad Kamil Yaakob [1,4],
Siti Irma Yuana Saaid [3], Umi Sarah Jais [1,2]

[1]Faculty of Applied Sciences, Universiti Teknologi MARA, 40450 Shah Alam, Selangor, Malaysia
[2]Metals,Ceramics and Composites Group, Materials Technology, Universiti Teknologi MARA, 40450 Shah Alam, Selangor, Malaysia
[3]Centre of Foundation Studies, Universiti Teknologi MARA, 42300, Puncak Alam, Selangor, Malaysia
[4]Institute of Science, Universiti Teknologi MARA, 40450 Shah Alam, Selangor, Malaysia
[1]E-mail: zulaikhasuhaili@gmail.com

ABSTRACT

Pure TiO_2 and Cr doped TiO_2 (0.1-1.0wt% Cr) nanoparticles were synthesized via sol gel method. This study focuses on narrowing the TiO_2 band gap energies in order to enhance the photocatalytic efficiency under visible light. The synthesized samples were characterized by X-Ray diffraction method (XRD), field emmision (FESEM) and also UV-Vis diffuse reflectance spectroscopy (DRS).The photocatalytic activity under sunlight irradiation was demonstrated by photocatalytic decomposition of methylene blue in water using UV/Vis spectrophotometer. The XRD analysis of pure TiO_2 and doped TiO_2 calcined at 500^{o}C showed a mixture of anatase and rutile phases with decreasing crystallites size from 13.3nm to 11.6nm as the concentration of Cr was increased. The anatase-rutile phase transformation increased from 28.8% to 57.4%. An indication shows that at 0.75wt%, Cr the anatase and rutile phases have equal composition percentage. This study demonstrated that band gap energy of TiO_2 was reduced with Cr doping which could enhance the photocatalytic efficiency. Sample containing 1.0wt% exhibit the lowest optical band gap energy at 2.86 eV. The optimum chromium doping concentration was found to be at 0.1 wt% Cr corresponding to band gap energy of 2.87 eV and degradation rate of 84%.

Keywords: *Sol-gel chemistry, optical properties, titanium dioxide, chromium; photocatalytic activity*

INTRODUCTION

Numerous organic compounds that are commonly used in industrial, agricultural, and domestic fields cause contamination to the environment. This frequent occurrence has received great attention on the investigation of photocatalysis to eliminate hazardous substances. In the preceding years photocatalytic technology has revealed to be a promising method to solve the environmental crisis since it is an economical and harmless technology [1-4]. Titanium dioxide is known as an efficient photocatalyst. It has received enormous interest due to it being inexpensive, non-toxic, and biocompatible that shows high photoefficiency and activity besides the capability to degrade gaseous and aqueous contaminants and hence is a good candidate for use in air clean-up and water purification [5-8].

However, titanium dioxide has a number of limitations in that the high energy band gap (ca. 3.0 eV for rutile and 3.2 eV for anatase) make it only possible to be activated by ultraviolet (UV) light [9, 10]. Modifications of titanium dioxide appeared necessary to improve the performance of the photocatalytic by doping with several metal ions in order to extend the absorption range of TiO_2 into the visible region. In fact, previous studies had proven that doping with transition metal ions resulted in improved performance of photocatalytic activity. Where these transitions metal ions such as Fe^{3+} , Y^{3+} and Mn^{2+} helped to boost the photocatalytic activity by trapping photo-generated electrons in TiO_2 or due to the genesis of reactive complexes that lifted the electron-hole pair lifetimes [11-13].

In this work, the photocatalytic activity in visible light of TiO_2 doped with varying amount of Cr were synthesized in alkaline medium and the optical property been studied. Herein, in this study we report on the synthesis of sol-gel TiO_2 with Cr metal ions where the photocatalytic will be done by using sunlight as the energy light source to improve the performance of the photocatalytic activity. To our knowledge, the effect of Cr as dopant for the photocatalytic activity of TiO_2 under direct sunlight excitation was not reported elsewhere. The few published data were concerned only with

photocatalytic activity under UV irradiation and visible light with various results depending on the type of dopant and preparation method.

EXPERIMENTAL

Sample Preparation

Chromium doped titania with increasing amount of chromium (0.1-1.0 wt%) were synthesized via sol gel method. The method was adopted with modification from Hong-bin Yang et al [14]. Absolute ethyl alcohol was mixed with titanium butoxide ($Ti(OBu)_4$) with a ratio of 5:2. The triethanolamine was added into the solution and constantly stirred for 15 minutes using an electromagnetic stirrer. Then, absolute ethyl alcohol and distilled water were added into the above solution with stirring. An increasing amounts of 0.1, 0.5 and 1.0 wt % of Cr^{3+} was added into a series of the above solutions. Stirring was continued for half an hour, stabilized and aged for 3 days at room temperature to form gel. The gel was dried at 80°C for 72 h, ground and calcined at 500°C for 4 h.

Characterisation

The analysis was performed using XRD spectrometer model Panalytical X'Pert PRO. The diffractometer data were recorded for 2Θ values in a range of 10° to 80°. The patterns were compared with JCPDS reference data for phase identification and crystallite size was calculated using Scherrer equation by referring the 2 most intense peaks of 101 and 110 show on the XRD diagram. The microstructure of the catalyst powder was determined by high resolution scanning electron microscopy (FESEM) model Carl Zeiss SMT, SUPRA'40 VP. UV-Vis NIR diffuse reflectance spectroscopy (DRS) was performed with a Shimadzu Cary 5000 UV-Vis-NIR spectrophotometer equipped with an integrating sphere to identify the optical band gap energy. The absorption edge value and the band gap energy can be computed based on the reflectance spectra. Photocatalytic activity of the Cr^{3+} doped catalyst was evaluated by measuring the intensity degradation of methylene blue aqueous solution under sunlight irradiation. The methylene blue (MB) was used as a model compound. In the experiment 0.1 g of the prepared catalyst powder with increasing Cr^{3+} doping was dispersed into a 50 ml of 10 ppm methylene blue solution with 10ppm concentration. This solution was

magnetically stirred in the dark for 30 minutes before exposure to sunlight to establish the adsorption-desorption equilibrium of the organic dye. The study was carried out under direct sunlight between 11 am and 2 pm with the average solar intensity at 500-600 W/m^2 which was measured by SEAWARD Solar Survey 100. The experiment was performed on the bright sunny day with temperature 32^{o}C.The first MB sample was taken at the end of the dark adsorption period just before the light was turned on and was treated as the starting point (t = 0). Aliquot samples were then withdrawn regularly at 30 minutes interval up to 180 minutes. The photocatalytic degradation reaction was determined by measuring the absorbance of the solution samples with UV-Vis spectrophotometer at λ_{max} of MB (622 nm). The photocatalytic degradation of MB was calculated from the following relationship:

$$\text{Degradation percent, } D\% = [(A_o - A_t) / A_o] \times 100\%$$

Where A_o is the initial absorbance of MB solution and A_t is the absorbance of MB solution at time t (minutes).

RESULTS AND DISCUSSION

Phase Analysis

Representatives the X-ray diffraction pattern of pure TiO_2 as dried at 80^{o}C for 72 h and calcined at 500^{o}C for 4 hours (h) and chromium doped TiO_2 photocatalyst calcined at 500^{o}C for 4h are shown in Figure 1. The as dried TiO_2 powder in Figure 1 is amorphous but crystallized to form rutile and anatase after 4h heat treatment at 500^{o}C. As can be seen, for all the samples appears in two polymorhic forms which are anatase and rutile. This results corroborate well with previous studies where Bouattour et al. also observed similar effect using Li^+ and Rb^+ as dopants [15]. However, anatase and rutile intensity changed when the dopant concentration changed. According to Figure 1, it can be seen at 0.5 and 1.0 wt% Cr the rutile intensity is also increased. However, at 0.1wt% Cr the anatase phase intensity is increased while the rutile phase intensity is decreased compared to the pure TiO_2, 0.5wt% Cr and 1.0wt% Cr. Contrary to our previous work on cerium doping, the addition of chromium fallouts into a reduction intensity peaks on the anatase phase [16]. At the prominent peak of 38.04^o the intensity of

anatase phase is decreased at 0.5wt% and 1.0wt% Cr dopant concentration. It could be inferred that the increase concentration of chromium caused anatase poorly crytallized. Based on the reference of anatase and rutile phases of TiO_2 (JCPDS 711166, 731765) the synthesized photocatalyts correspond to tetragonal crystal system having space group of I41/amd and P42/mnm respectively. Based on Figure 1, the XRD peaks broaden when the chromium concentration is at 0.5wt% and 1.0wt%. This could be inferred to the crystallization of anatase nanopowders diminished and accompanied by a decrease in the crystallite size of Cr doped TiO_2. This can be proven by the result displayed in Table 1 where the crystallite sizes of the anatase phase are reduced from 13.3 nm for pure TiO_2 to 12.1nm and 11.6 nm for the dopant concentration at 0.5wt% Cr and 1.0wt% Cr respectively. Peng et al believed that the reduction in grain size could be ascribed to the existence of Cr-O-Ti, which hindered the coalescence of the neighboring grains suppressing the growth of anatase rutile crystals throughout the heat treatment process [17]. This is dissimilar to that of 0.1wt% Cr where the crystallite size is 13.5 nm which is 0.2 nm greater than pure TiO_2.

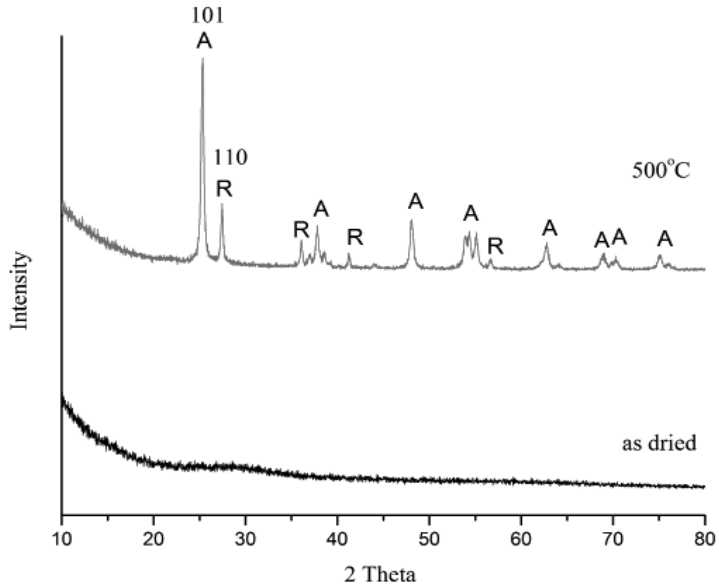

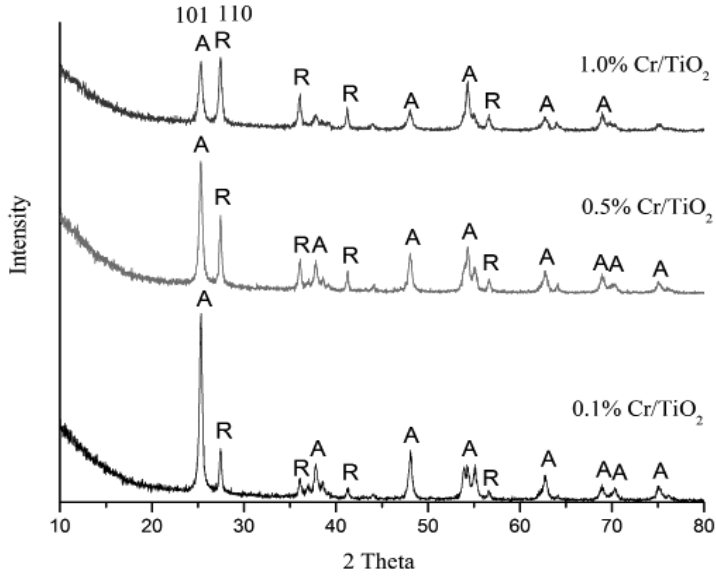

Figure 1: XRD patterns of pure TiO_2 and Cr-doped TiO_2

Table 1: Anatase-Rutile composition and crystallite size of pure TiO_2 and Cr-doped TiO_2

Samples	Anatase X_A%	Rutile X_R%	Ratio X_A%/ X_R%	Crystallite size (nm)
TiO_2	71.8	28.2	2.55	13.3
0.1wt% Cr/ TiO_2	73.9	26.1	2.83	13.5
0.5wt% Cr/ TiO_2	57.1	42.9	1.33	12.1
1.0wt% Cr/ TiO_2	42.6	57.4	0.74	11.6

The mass fraction of rutile in Figure 2 was calculated based on the formula developed by Spurr and Myers [18]. Pure TiO_2 consists of 28.2% of rutile phase while at 0.1wt% Cr, 0.5wt% Cr and 1.0wt% Cr the percentage of rutile phase is at 26.1%, 42.9% and 57.4% respectively. The rutile percentage is decreased at 0.1wt% Cr but the rutile percentage is increased at 0.5wt% and 1.0wt% Cr. This percentage composition of rutile phase elucidating that at higher Cr doping did not inhibit the formation of rutile phase and stabilize the anatase phase at 500°C calcined temperature. It is

noted at 0.75wt% Cr doping resulted in 50:50 of anatase and rutile phase which is shown at intersection point depicted in Figure 2.

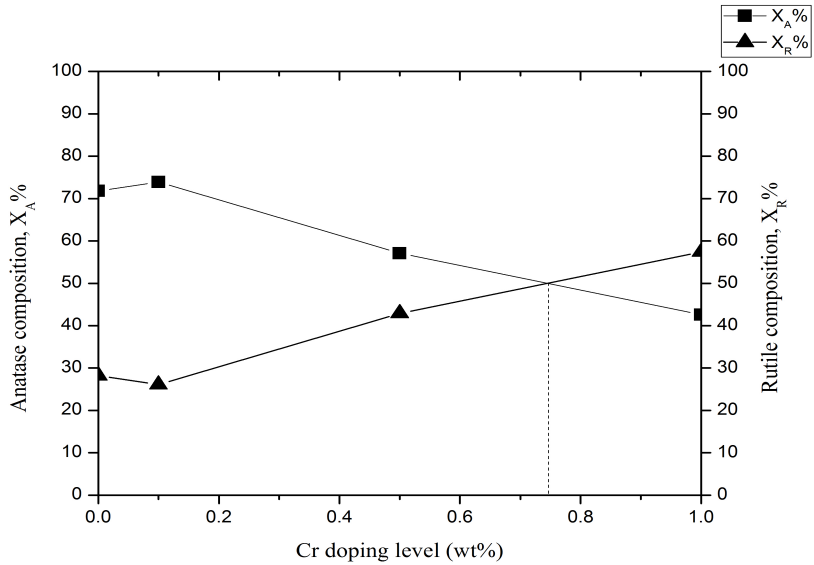

Figure 2: Proportion of anatase and rutile of pure TiO_2 and Cr-doped TiO_2

MICROSTRUCTURAL ANALYSIS

Figure 3 shows the FESEM micrographs of the pure TiO_2 and Cr doped TiO_2 nanopowders. The microstructure of pure TiO_2 nano powders consists of large spherical particles. However, the morphology of chromium doped TiO_2 nanopowders show that conjugated spherical particles become smaller as the Cr concentration increased.

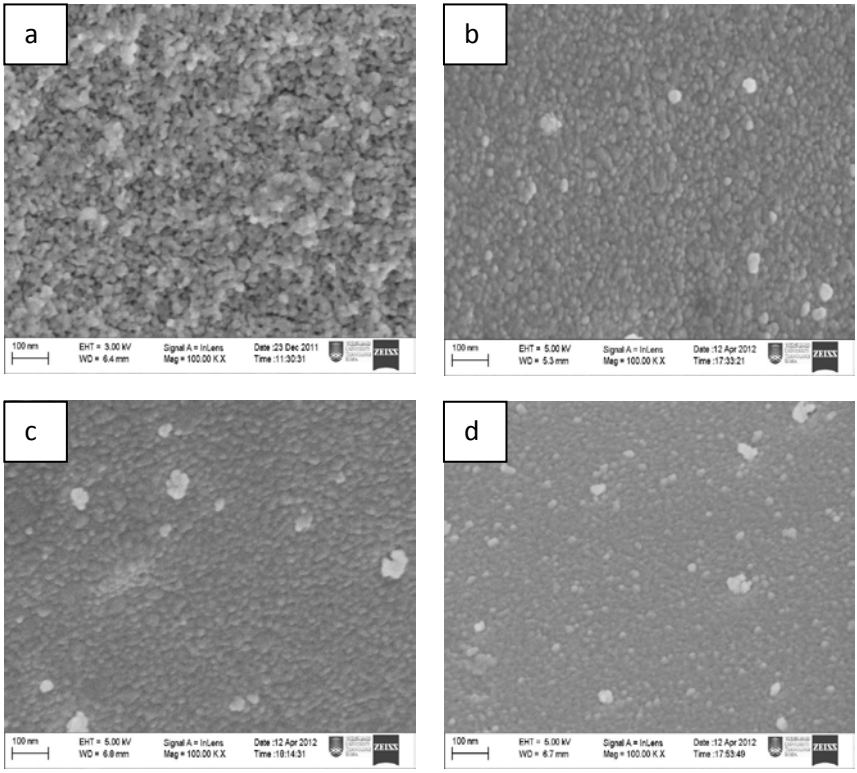

Figure 3: FESEM of pure TiO_2 and Cr-doped TiO_2

OPTICAL PROPERTIES

The diffused reflectance spectra in the Cr doped TiO_2 powders are supplemented by the colour change in from white, to yellow to dark green when the Cr^{3+} concentration increased. The corresponding diffused reflectance spectra are shown in Figure 4. The diffused reflectance spectra shift towards longer wavelength as Cr concentration increased. The absorption spectra F(R) were computed by adopting the Kubelka-Munk equation, $F(R) = (1 - R)^2/2R$ where R is the diffused reflectance of the samples [19].

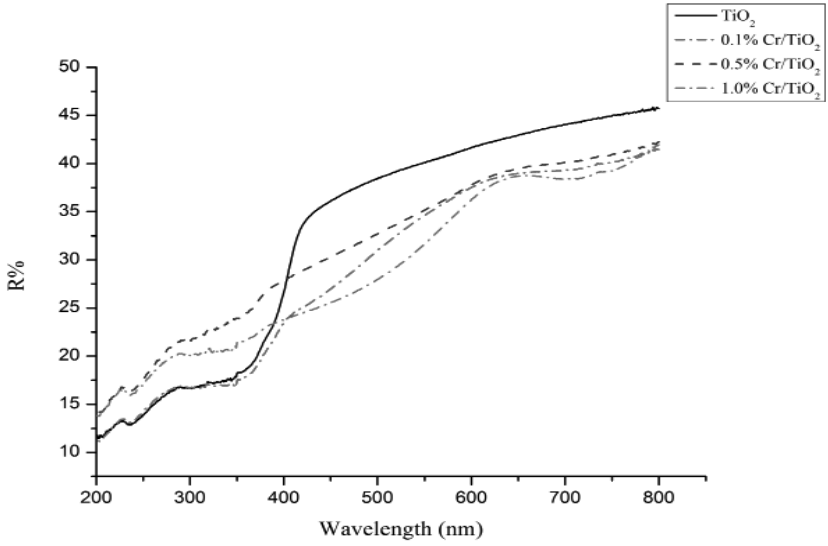

Figure 4: Diffuse reflectance spectra of pure TiO_2 and Cr-doped TiO_2

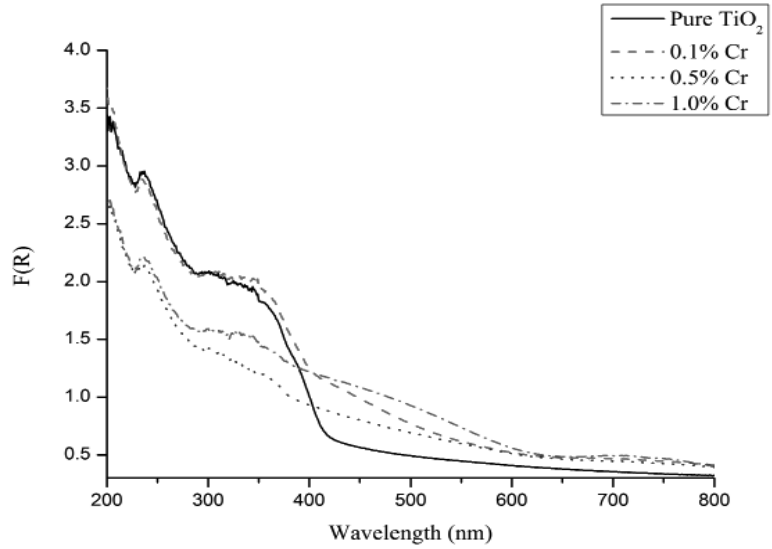

Figure 5: Kubelka-Munk absorption curves of pure TiO_2 and Cr-doped TiO_2

The corresponding kubelka-munk absorption curves of pure TiO_2, 0.1wt% Cr, 0.5wt% Cr and 1.0wt% Cr are illustrated in Figure 5. It is demonstrated in the absorption spectra that pure TiO_2 depicts one only absorption peak near to 350 nm. On the other hand, Cr doped TiO_2 samples exhibit an absorption peak around 350 nm and one broad peak in the range of 400 and 600. The peak at 350 nm occurred because of the phonon assisted indirect transition from the edge to the center of Brilliouin zone [20]. While the broad peak at 400-600 nm is due to $^4A_2$ (F) to $^4T_1$ (F) transition. The other peak is in the range of 600–800 nm wavelength occured due to spin forbidden $^4A_2$ (F) to ^2E, $^2T_1$ transition. Chromium ions were claimed to show these types of d–d electronic transition when it is in +3 oxidation states, under the influence of octahedral crystal field. In anatase TiO_2, Ti^{4+} is surrounded by six oxygen ions forming TiO_6^{2-} octahedra. When Cr^{3+} occupies Ti^{4+} in the lattice, it may form CrO_6. In that condition, it is under the ligand field environment of six O^{2-} ions. Due to the repulsion between the electrons present in Cr^{3+} and O^{2-} ion, the energy of d orbital is splitted up giving ground state $^4A_2$ and excited states $^4T_1$, $^4T_2$, ^2E. Absorption of UV–vis light excites the electrons from ground state to different excited states giving aforementioned d–d absorption peaks. The d–d transition of Cr^{3+} in TiO_2 is shown in the inset of Figure 5 [21]. Hence for futher conformation, the optical band gap energy was determined by extrapolation of the tangent to the inflexion point between the absorption tail and the band states where $\alpha = 0$ from the Tauc plot in Figure 6.The tauc plot was applied based on the Tauc relation using the following equation:

$$\alpha = A(h\nu - E_g)^n / h\nu,$$

Where α is absorption coefficient, A is constant, $h\nu$ is the energy of light and n is a constant depending on the nature of the electron transition modes (n = ½ for direct allowed transitions)[22, 23]. The reduction in the band gap energy can be observed as the chromium impurities been added. The bare TiO_2 energy band gap was found to be at 2.97 eV. This value is relatively lower from the bulk TiO_2; (Anatase Eg = 3.2 eV, Rutile Eg = 3.0 Ev). While 2.87 eV, 2.91 eV and 2.86 eV for 0.1, 0.5 and 1.0 wt% Cr respectively. This can be understood sample at 1.0wt% Cr containing highest rutile phase (Table 1) has lowest band energy because rutile band gap energy is lower than anatase band gap energy. Previous study reported that distortion in energy band contribute in alteration of the absorbance spectral characteristic[24].

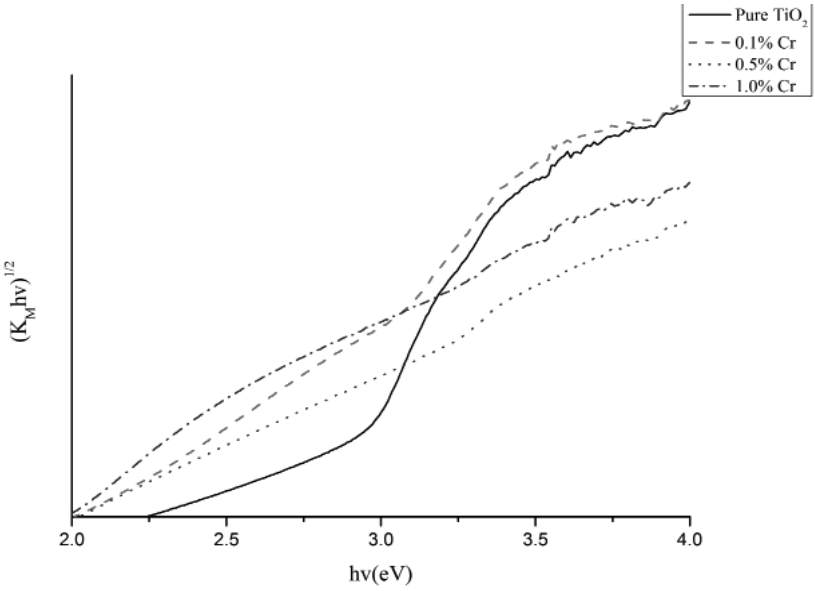

Figure 6: Tauc plot of pure TiO_2 and Cr-doped TiO_2

PHOTOCATALYTIC ACTIVITY

Figure 7 shows the degradation of methylene blue against irradiation time in the presence of the sunlight irradiation. The performance of the photocatalytic activity increased when the composition of anatase phase is greater than the rutile phase. The percentage of the reduction of methylene blue are 41%, 84%, 72%, 70% for pure TiO_2, 0.1wt% Cr/TiO_2, 0.5w% Cr/TiO_2 and 1.0wt% Cr/TiO_2 respectively. Based on Figure 6, Cr doping shows a significant influence on the certain properties of the TiO_2. Whereby Cr doped TiO_2 upon an increasing Cr concentration were investigated throughout the following characteristics: (i) the anatase-to-rutile transformation, (ii) decrease of the rutile crystallite size, (iii) increase of visible light absorption and finally, (iv) photocatalytic efficiency. This can be explained by an improved visible light absorption which may allow an improved charge carrier separation in the synthesized samples of Cr doped TiO_2 and acting as electron traps. However, the decrease of the photocatalytic performance for higher Cr loading can be explained by an improved charge carrier

recombination due to a high defect concentration, small rutile crystallite size and low anatase content [28]. As can be observed in Figure 7, 0.1wt% shows the best performance photocatalytic activity because of higher anatase content compared to pure TiO_2, 0.5wt% and 1.0wt% Cr doped TiO_2. This indicated that 0.1% Cr doped TiO_2 is an optimal doping level for photocatalysis under visible sunlight. The crystallite size of anatase phase also show 0.1wt% is the largest compared to pure TiO_2, 0.5wt% Cr and 1.0wt% Cr.This is in a good agreement which anatase has been known as a photoactive phase.

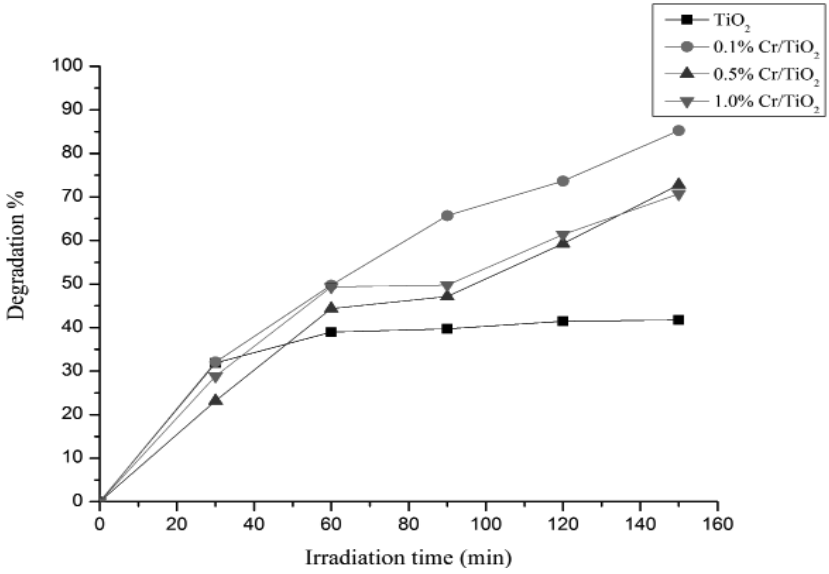

Figure 7: Degradation of methylene blue of pure TiO_2 and Cr-doped TiO_2

CONCLUSION

Pure TiO_2 and chromium doped TiO_2 were synthesized via sol-gel route ranging from 0.1 - 1.0 wt% Cr. The XRD analysis of pure TiO_2 and doped TiO_2 calcined at 500^{o}C showed a mixture of anatase and rutile phases with decreasing crystallites size as the concentration of Cr was increased. This study demonstrated that energy band gap of TiO_2 was reduced with Cr doping which could enhance the photocatalytic efficiency. The optimum

chromium doping concentration after synchronizing the experimental data with that of theoretical data was found to be 0.1 wt% corresponding to band gap energy of 2.87 eV and degradation rate of 84%.

ACKNOWLEDGEMENT

The authors are gratefully thanks to Ministry of Education (MOE) for supporting this research under the RAGS grant (600-RMI/RAGS 5/3 (26/2012)), and Universiti Teknologi MARA (UiTM) for the facilities provided in succeeding this research.

REFERENCES

[1] J. Xie, D. Jiang, M. Chen, D. Li, J. Zhu, X. Lü, and C. Yan, 2010. Preparation and characterization of monodisperse Ce-doped TiO_2 microspheres with visible light photocatalytic activity, *Colloids and Surfaces A: Physicochemical and Engineering Aspects*, *372*(1–3), pp. 107-114.

[2] A. Alem, H. Sarpoolaky, and M. Keshmiri, 2009. Sol-gel preparation of titania multilayer membrane for photocatalytic applications, *Ceramics International*, *35*(5), pp. 1837-1843.

[3] Saepurahman, M. A Abdullah, and F.K Chong, 2010. Preparation and characterization of tungsten-loaded titanium dioxide photocatalyst for enhanced dye degradation', *Journal of Hazardous Materials*, *176*(1–3), pp. 451-458.

[4] A. Alem, and H. Sarpoolaky, 2010. The effect of silver doping on photocatalytic properties of titania multilayer membranes, *Solid State Sciences*, *12*(8), pp. 1469-1472.

[5] C.C Pan, and J.C.S Wu, 2006. Visible-light response Cr-doped TiO_2−XNX photocatalysts, *Materials Chemistry and Physics*, *100*(1), pp. 102-107.

[6] M. Behpour, and V. Atouf, 2012. Study of the photocatalytic activity of nanocrystalline S, N-codoped TiO_2 thin films and powders under visible and sun light irradiation, *Applied Surface Science*, *258*(17), pp. 6595-6601.

[7] M. Keshmiri, M. Mohseni, and T. Troczynski, 2004. Development of novel TiO_2 sol-gel-derived composite and its photocatalytic activities for trichloroethylene oxidation, *Applied Catalysis B: Environmental*, *53*(4), pp. 209-219.

[8] A. Fujishima, X. Zhang, and D.A Tryk, 2007. Heterogeneous photocatalysis: From water photolysis to applications in environmental cleanup, *International Journal of Hydrogen Energy*, *32*(14), pp. 2664-2672.

[9] Q. Ling, J. Sun, Q. Zhou, and H. Ren, 2008. Visible-light-driven boron/ferrum/cerium/titania photocatalyst, J*ournal of Photochemistry and Photobiology A: Chemistry*, *200*(2–3), pp. 141-147.

[10] C. Suwanchawalit, S. Wongnawa, P. Sriprang, and P. Meanha, 2012. Enhancement of the photocatalytic performance of Ag-modified TiO_2 photocatalyst under visible light, *Ceramics International*, *38*(6), pp. 5201-5207.

[11] H. Zhang, G. Miao, X. Ma, B. Wang, and H. Zheng, 2014. Enhancing the photocatalytic activity of nanocrystalline TiO_2 by co-doping with fluorine and yttrium, *Materials Research Bulletin*, *55*(0), pp. 26-32.

[12] J.A Navío, J.J Testa, P. Djedjeian, J.R Padrón, D. Rodríguez, and I.M Litter, 1999. Iron-doped titania powders prepared by a sol-gel method.: Part II: Photocatalytic properties, *Applied Catalysis A: General*, *178*(2), pp. 191-203.

[13] H.S.M Tabaei, M. Kazemeini, and M. Fattahi, 2012. Preparation and characterization of visible light sensitive nano titanium dioxide photocatalyst, *Scientia Iranica*, *19*(6), pp. 1626-1631.

[14] Y. Hong-bin, W. Wen ke, J. Xiu-yan, and Y. Sheng-ke, (2010, edn.). Preparation of Doped Nano-TiO_2 by Sol-Gel Method and the study on Its Photocatalytic Performance, in Editor (Ed.)^(Eds.): Book Preparation of Doped Nano-TiO_2 by Sol-Gel Method and the study on Its Photocatalytic Performance, pp. 1-4.

[15] S. Bouattour, A.M Botelho do Rego, and L.F Vieira Ferreira, 2010. Photocatalytic activity of Li^+–Rb^+–Y^{3+} doped or codoped TiO_2 under sunlight irradiation, *Materials Research Bulletin*, *45*(7), pp. 818-825.

[16] S.Z Suhaili, and U.S Jais, (2012, edn.). Improved visible light photocatalytic activity of TiO_2 nano powder by Ce doping, in Editor: Book Improved visible light photocatalytic activity of TiO_2 nano powder by Ce doping, pp. 743-747.

[17] Y.H Peng, G.F Huang, and W.Q Huang, 2012. Visible-light absorption and photocatalytic activity of Cr-doped TiO_2 nanocrystal films, *Advanced Powder Technology*, *23*(1), pp. 8-12.

[18] R.A Spurr, and H. Myers, 1957. Quantitative Analysis of Anatase-Rutile Mixtures with an X-Ray Diffractometer, *Analytical Chemistry, 29*(5), pp. 760-762.

[19] A.A Christy, O.M Kvalheim, and R.A Velapoldi, 1995. Quantitative analysis in diffuse reflectance spectrometry: A modified Kubelka-Munk equation', *Vibrational Spectroscopy*, *9*(1), pp. 19-27

[20] N. Serpone, D. Lawless and R. Khairutdinov, 'Size Effects on the Photophysical Properties of Colloidal Anatase TiO_2 Particles: Size Quantization versus Direct Transitions in This Indirect Semiconductor, *The Journal of Physical Chemistry*, *99*(45), pp. 16646-16654.

[21] B. Choudhury, and A. Choudhury, 2013. Structural, optical and ferromagnetic properties of Cr doped TiO_2 nanoparticles, *Materials Science and Engineering: B*, *178*(11), pp. 794-800.